Supplementary Information

Ni-Co-O hole transport materials: gap states assisted hole extraction with enhanced electrical conductivity

Yu Hou,[†a] Li Juan Tang,[†a] Hong Wei Qiao,[a] Zi Ren Zhou,[a] Yu Lin Zhong,[c] Li Rong Zheng,[d] Meng Jiong Chen,[a] Shuang Yang,*[b] Hua Gui Yang*[a]

[a]*Key Laboratory for Ultrafine Materials of Ministry of Education, School of Materials Science and Engineering, East China University of Science and Technology, 130 Meilong Road, Shanghai 200237, China*

[b]*Key Laboratory for Liquid-Solid Structural Evolution and Processing of Materials, Ministry of Education, School of Materials Science and Engineering, Shandong University, Jinan, 250061, P. R. China*

[c]*Centre for Clean Environment and Energy, Gold Coast Campus, Griffith University, Queensland 4222, Australia*

[d]*Beijing Synchrotron Radiation Facility, Institute of High Energy Physics, Chinese Academy of Sciences, Beijing, 100049, China*

[†]These authors contributed equally to this work.

Correspondence and requests for materials should be addressed to Shang Yang (syang@sdu.edu.cn) and Hua Gui Yang (hgyang@ecust.edu.cn).

Methods

Substrate treatment. The patterned FTO-coated glass substrates were cleaned using ultrasonication in detergent, acetone, ethanol and deionized water, and then dried at 80 ^{o}C, followed by UV ozone treatment for 15 min.

Preparation of Ni-Co-O films. Typically, 0.05925 g $NiCl_2 \cdot 6H_2O$, 0.1185 g $CoCl_2 \cdot 6H_2O$ and 0.21 g citric acid monohydrate were dissolved into 3.5 mL N, N-Dimethylformamide (DMF, 99.9%, Alfa Aesar) under constant magnetic stirring to form a clear solution[1]. Different precursor solutions for Co content were prepared by dissolving different qualities of $NiCl_2 \cdot 6H_2O$ and $CoCl_2 \cdot 6H_2O$ with the total concentration of metal ions to be 0.214 M. The solutions were then spin-coated onto FTO at 4000 rpm for 60 s, followed by heated at 100 ^{o}C for 10 min, after cooling to room temperature, the films were calcined at 400 ^{o}C for 1 h.

Synthesis of methylammonium iodide (CH_3NH_3I). The CH_3NH_3I was prepared according to a reported method[2]. CH_3NH_3I was synthesized by reacting 27.86 mL methylamine (40% in ethanol, Sigma-Aldrich) and 30 mL hydroiodic acid (57 wt% in water, Sigma-Aldrich) in a 250 mL round-bottomed flask at 0 ^{o}C for 2 h with stirring. The precipitate was recovered by evaporation at 50 ^{o}C for 1 h. The product was dissolved in ethanol, recrystallized from diethyl ether and dried at 60 ^{o}C in a vacuum oven for 12 h. The white powder was collected and stored under argon atmosphere before use.

Device Fabrication. PbI_2 (DMSO) complex solution in DMF was prepared by mixing 0.5993 g PbI_2 (99.9985%, Alfa Aesar), 92 μL dimethylsulfoxide (DMSO, 99.9%, Sigma-Aldrich), 1 mL DMF with stirring at room-temperature overnight. The PbI_2 (DMSO) solution was spin-coated on hole transport layers (HTLs) at 3000 rpm for 30 s, and then MAI solution (60 mg/mL in 2-propanol) was spin-coated on the top of the transparent PbI_2 (DMSO) film at 5000 rpm for 30 s. The films changed to dark brown during spin coating and the films were dried on a hot plate at 100 ^{o}C for 10 min. Then, PCBM (20 mg/mL in chlorobenzene) and BCP (0.5 mg/mL in ethanol) were deposited

by spin coating at 2000 rpm for 45 s, and 4000 rpm for 45 respectively. Finally, 110 nm of Ag was thermally evaporated as the back electrode.

Characterization. The morphology and structure of the HTLs were characterized by field emission scanning electron microscopy (FESEM, HITACHI S4800). The X-ray diffraction (XRD) spectra of the prepared HTLs were measured using powder XRD (Bruker D8 Advanced Diffractometer, Cu Kαradiation, 40kV). X-ray photoelectron spectroscopy (XPS, PHI5300, Mg anode, 250 W, 14 kV) was used to analyze the elemental composition of the HTLs. The work functions were measured by ultraviolet photoelectron spectrum (UPS) with He source of incident energy of 21.21 eV (He I line). The transmittance spectra of HTLs and the absorption spectra of the perovskite were measured by using a Cary 500 UV-Vis-NIR Spectrophotometer. The photoluminescence measurement was acquired at room temperature with a UV-Vis-NIR fluorescence spectrophotometer (Fluorolog-3-P) with an excitation wavelength of 515 nm. The solar cells were illuminated using a solar light simulator (Solar IV-150A, Zolix) and the power of the simulated light was calibrated to 100 mW cm^{-2} using a Newport calibrated KG5-filtered Si reference cell. *J-V* curves of solar cells were measured using a Keithley 2400 digital sourcemeter. Devices were masked with a metal aperture to define the active area to be 0.0625 cm^{-2}. The stead state current output of the best-performing devices was measured by biasing the device at maximum power point for 100 s. The external quantum efficiency (EQE) was measured using a Newport-74125 system (Newport Instruments). The electrochemical impedance spectroscopy (EIS) was carried out on Electrochemical Workstation (Parstat 2273, Princeton) in the frequency range between 1 MHz and 100 Hz under short circuit at different bias. XAFS measurements were performed at the beam line 1W1B in Beijing Synchrotron Radiation Facility, China.

Supplementary Figures

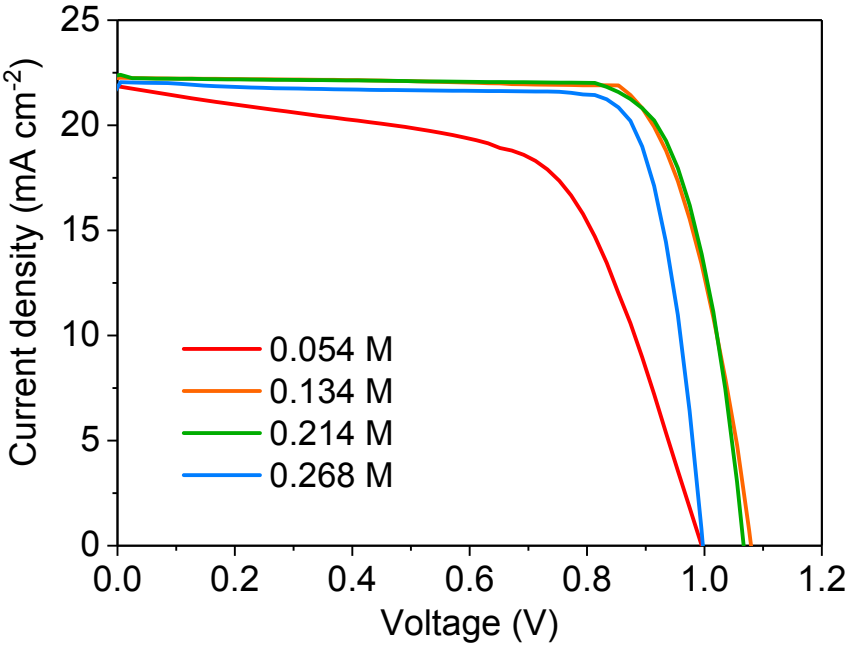

Fig. S1 *J-V* curve of the $NiCoO_x$ based device recorded at a scan rate of 0.15 V s^{-1}. The concentration of all metal ions in precursor is 0.214 M.

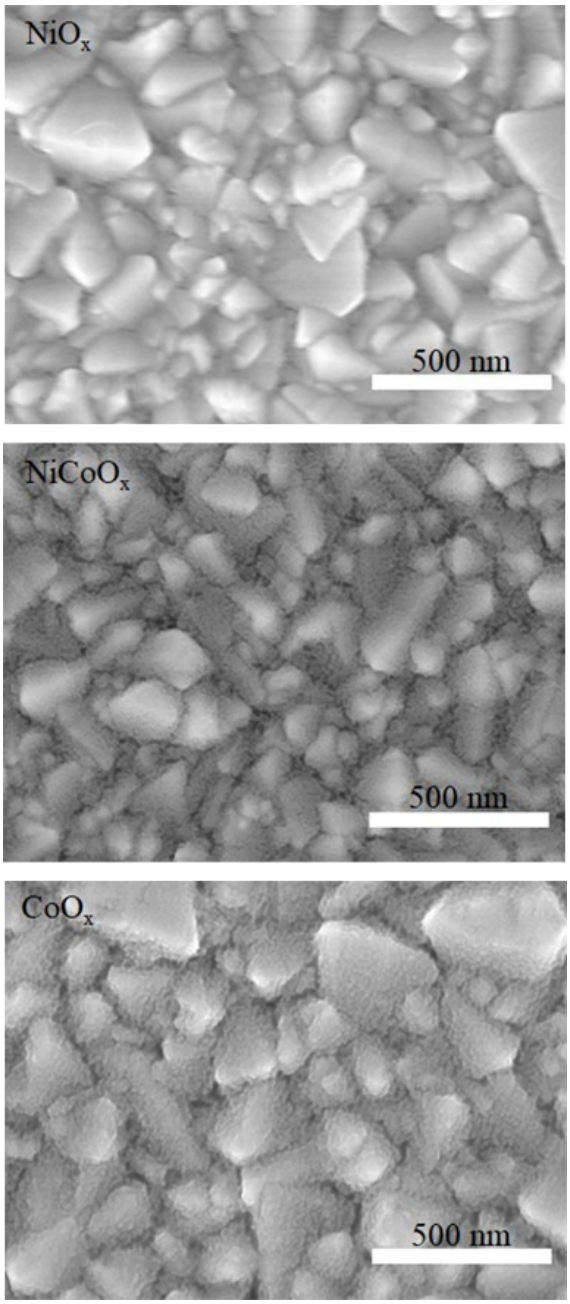

Fig. S2 Top-view SEM micrographs of NiO_x, $NiCoO_x$ and CoO_x layers deposited on FTO/glass. All films show essentially compact morphologies with full coverage of the FTO surface.

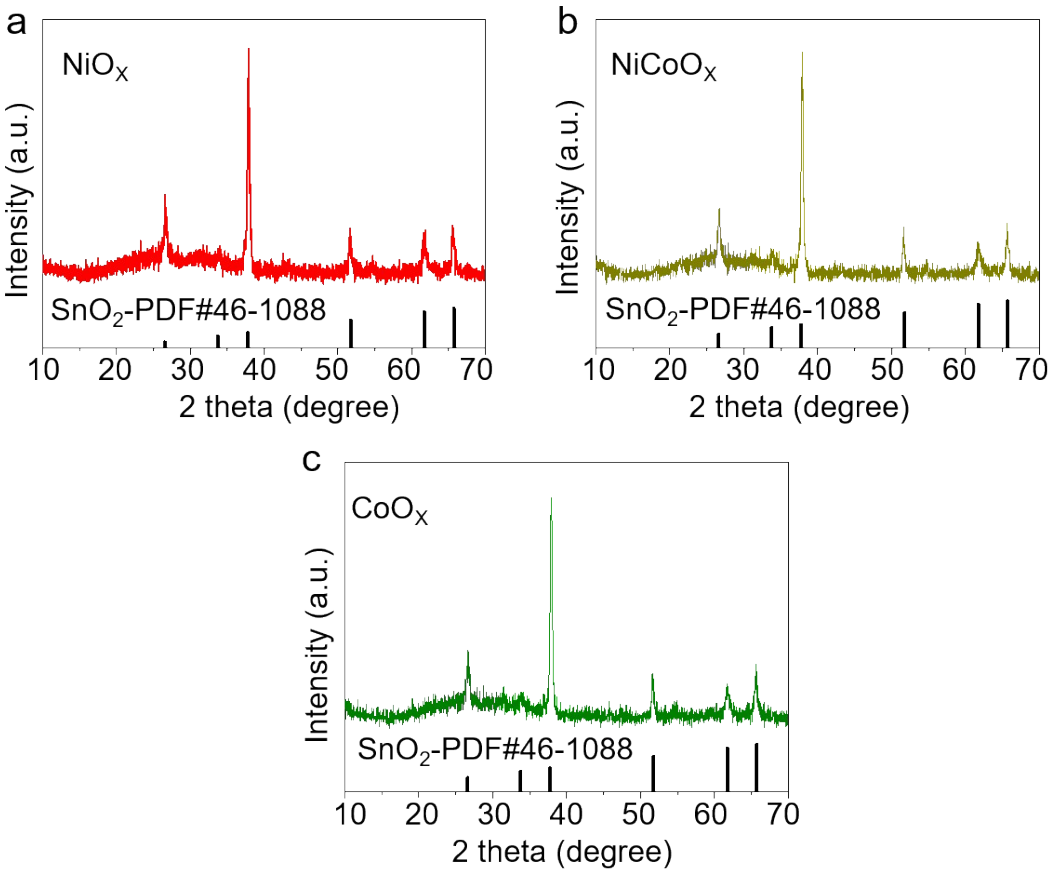

Fig. S3 XRD pattern of NiO_x, $NiCoO_x$ and CoO_x films deposited on FTO/glass.

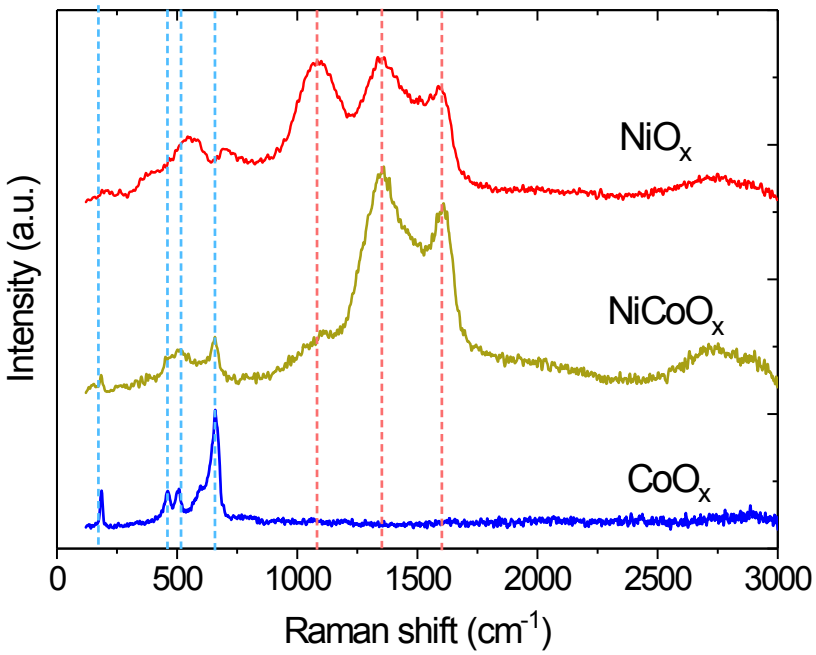

Fig. S4 Raman spectra of NiO_x, $NiCoO_x$ and CoO_x films. The NiO_x film shows there Raman bands at 1076, 1351 and 1606 cm^{-1}, while the CoO_x presents four Raman active bands at 189, 455, 513 and 660 cm^{-1}. The $NiCoO_x$ film displays the typical Raman bands of both films, indicating their structural similarity.

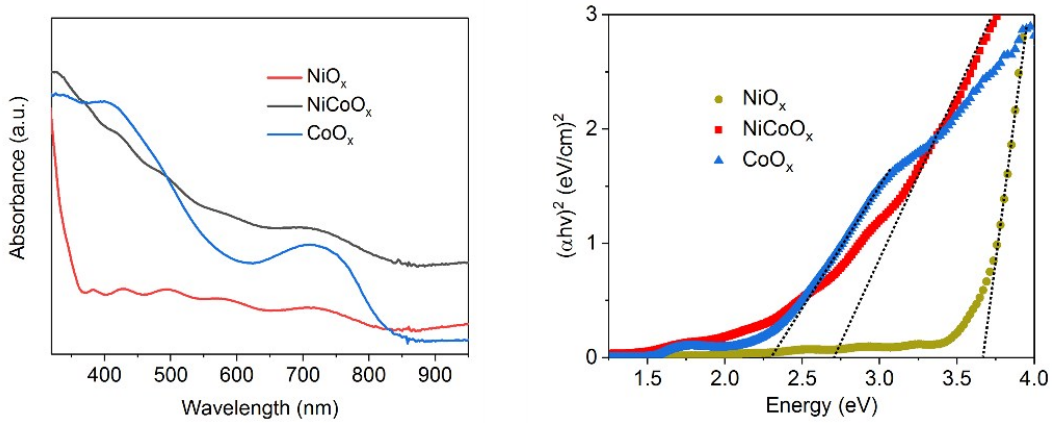

Fig. S5 UV-vis spectra (left) and Tauc plots (right) of NiO_x, $NiCoO_x$ and CoO_x films.

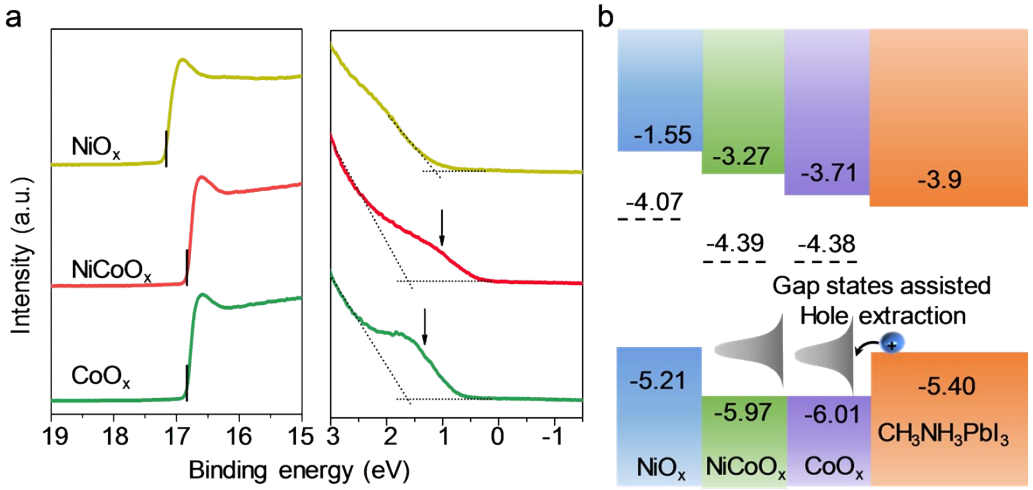

Fig. S6 (a) UPS spectra of the cut-off ($E_{cut\text{-}off}$) energy boundary (left) and valence band (VB) structure (right) of the NiO_x, $NiCoO_x$ and CoO_x films. All samples were deposited on FTO substrates. The VB tails (right figure) indicated by arrows are gap states within the bandgap of $NiCoO_x$ and CoO_x films. (b) Energy-level diagrams of the HTLs and perovskite (relative to the vacuum level). The dashed line shows the fermi level of the hole conducting materials deposited on FTO glass determined by UPS measurements. The occurrence of gap states in $NiCoO_x$ and CoO_x could provide electronic pathways for hole transfer from perovskites.

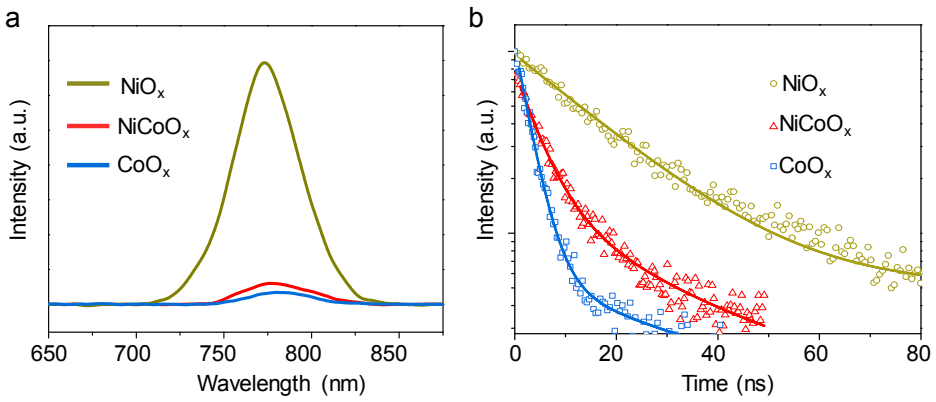

Fig. S7 (a) steady-state and (b) time-resolved photoluminescence (TRPL) decay of perovskite films with different HTLs.

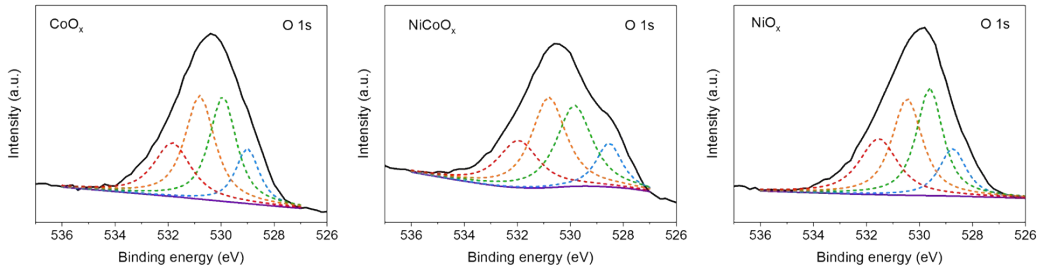

Fig. S8 O 1s XPS spectra of NiO_x, $NiCoO_x$ and CoO_x. The black and purple solid lines are raw XPS data and background, respectively. The dotted curves are the fitting of experimental data, which can be divided into O1 (red dotted line), O2 (orange dotted line), O3 (green dotted line) and O4 (blue dotted line) for all samples.

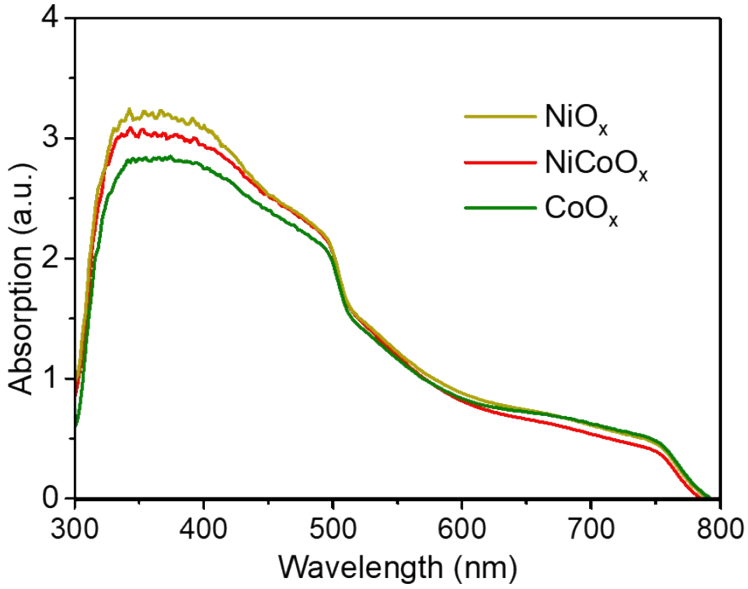

Fig. S9 Spectral absorbance of the perovskite films based on NiO_x, $NiCoO_x$ and CoO_x HTLs, showing their similar light absorbance efficiency between 300-800 nm.

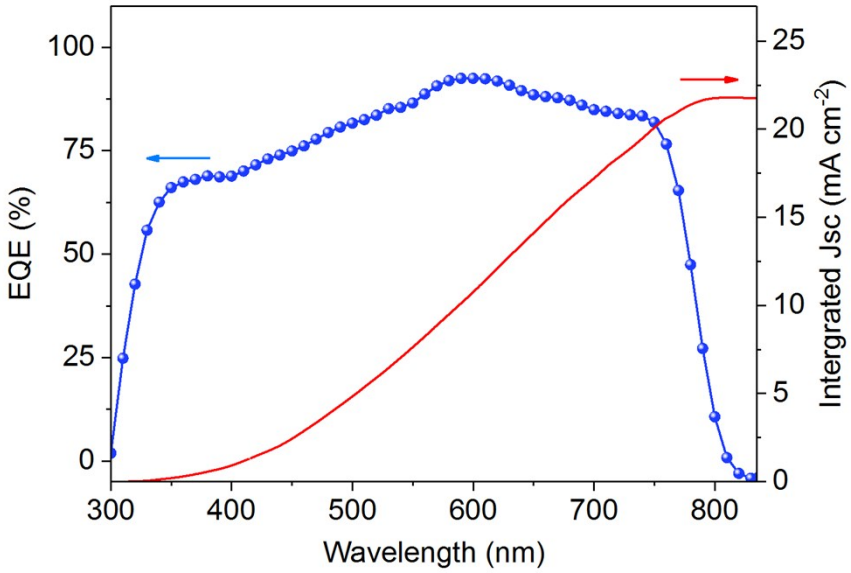

Fig. S10 EQE spectra for a typical perovskite solar cell based on $NiCoO_x$ HTLs.

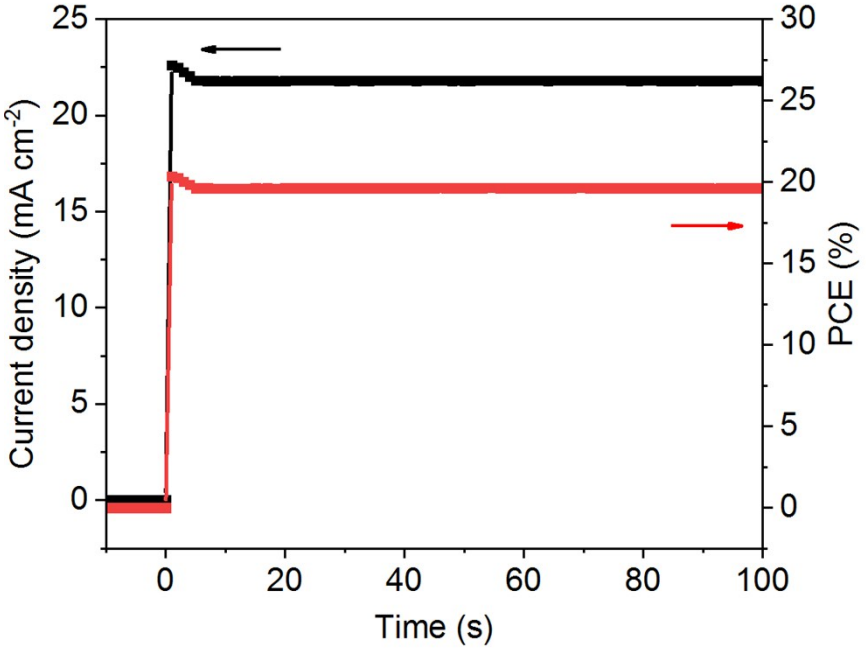

Fig. S11 Steady-state photocurrent and power output at maximum power point (MPP).

Table S1. Photovoltaic parameters of PSCs based on $NiCoO_x$ films with different Co contents.

$NiCoO_x$ (Co contents)		J_{SC} (mA/cm^2)	V_{OC} (V)	FF	PCE(%)
0%	Highest	22.71	1.035	0.730	17.14
	Average	22.66	1.038	0.699	16.48
25%	Highest	21.95	1.045	0.780	17.89
	Average	21.96	1.039	0.768	17.53
50%	Highest	22.27	1.080	0.833	20.03
	Average	22.09	1.068	0.785	18.51
75%	Highest	22.40	0.960	0.800	17.12
	Average	22.29	0.943	0.769	16.17
100%	Highest	21.65	0.987	0.465	9.95
	Average	20.55	0.974	0.452	9.04

References

[1] Chen, S., Yang, G., Jia, Y. & Zheng, H., Three-dimensional $NiCo_2O_4$@$NiWO_4$ core–shell nanowire arrays for high performance supercapacitors. *J. Mater. Chem. A* **5**, 1028-1034 (2017).

[2] Hou, Y. *et al*. A band-edge potential gradient heterostructure to enhance electron extraction effciency of the electron transport layer in high-performance perovskite solar cells. *Adv. Funct. Mater.* **27**, 1700878 (2017).